Cardiac Ultrasound Tomography Using Transducer With Sparse Elements and Anisotropic Regularization

Roberto C Ceccato[1], Chi-Nan Pai[1] , Sergio S Furuie[1]

[1] Escola Politécnica, Universidade de São Paulo, São Paulo, Brazil

Abstract

Quantitative time of flight in echo mode ultrasound computed tomography (TFEM USCT) is a highly ill-posed and typically ill-conditioned inverse problem, where the goal is to reconstruct the speed-of-sound (SoS) distribution from time-of-flight measurements. Compared to the more established transmission-mode USCT methods, TFEM USCT poses an even greater challenge due to increased indeterminacy, as the travel paths of the ultrasound signals are not well defined. As such, regularization is essential for achieving stable and physically meaningful reconstructions. This numerical study proposes an anisotropic variation of Tikhonov regularization using a second-derivative operator to account for directional SoS variations, with the aim of imaging the entire cardiac region using a single sparse linear transducer. The results demonstrate that the anisotropic regularization approach outperforms its isotropic counterpart, especially in preserving anatomical structures such as the myocardium and ventricle cavities. Moreover, the findings suggest that quantitative imaging of the cardiac region with a sparse transducer is feasible.

1. Introduction

Conventional ultrasound imaging is typically performed in B-mode, providing qualitative images for clinical interpretation. However, B-mode imaging is limited not only by its qualitative nature but also by the presence of artifacts and aberrations. These issues largely stem from the assumption of a homogeneous speed of sound (SoS) distribution when mapping reflections caused by spatial variations in acoustic impedance [1]. To address these limitations, time-of-flight echo-mode ultrasound computed tomography (TFEM USCT) has emerged as a promising alternative. This technique enables quantitative tissue characterization [2–5] and enhances B-mode reconstructions by providing more accurate SoS distributions, which serve as improved inputs for B-mode imaging [1].

Previous studies have primarily employed conventional small linear or phased transducers to image localized regions of interest (ROIs). This approach allows the use of standard ultrasound frequencies while avoiding phase-wrapping effects [4]. In contrast, the present numerical study investigates the use of a sparse hypothetical transducer designed to cover the entire cardiac region simultaneously. Such a configuration could enable rapid imaging of the whole heart, minimizing operator dependence by eliminating the need to reposition the transducer for different views. This would facilitate comprehensive cardiac imaging while preserving anatomical context.

Moreover, TFEM USCT inherently holds an ill-posed inverse problem [4], often resulting in ill-conditioned systems. Therefore, regularization techniques are crucial to ensure convergence and to obtain physically meaningful reconstructions. Tikhonov regularization with a Laplacian operator offers a robust solution to this challenge, particularly in noisy or data-limited settings. The Laplacian is computationally efficient, its application reduces to a single matrix multiplication, and it provides smooth reconstructions suitable for medical imaging. Additionally, the associated cost function yields linear first- and second-order derivatives, enabling the use of stable iterative solvers such as the Conjugate Gradient for Least Squares (CGLS) algorithm.

Despite these advantages, the standard Laplacian imposes isotropic smoothing, applying uniform regularization across all spatial directions. In cases where the SoS distribution exhibits anisotropic features, such as strongly layered media or adjacent regions with sharp contrast, this isotropic approach may be suboptimal. Additionally, it is well established that axial and lateral resolutions differ in pulse-echo ultrasound imaging, suggesting that direction-dependent regularization weights may provide improved reconstruction performance. To address this limitation, several studies have explored anisotropic regularization using first-order derivatives operators with Total Variation [3,5,6] or Tikhonov [2,4] regularization. While effective in promoting edge preservation, these methods often compromise numerical stability and smoothness, which are inherent advantages of second-order operators like the Laplacian.

In this study, an anisotropic extension of Laplacian-based Tikhonov regularization is proposed. The

herein proposed approach retains the numerical stability and smoothing properties of second-order regularization while introducing directional adaptivity to better capture anisotropic structures in TFEM USCT reconstructions.

2. Theory

In this study, the adaptive aperture strategy based on diverging waves is implemented as the time delay estimation (TDE) method. Following previous work [5], the least-squares formulation for the TFEM USCT inverse problem in this TDE approach can be expressed as

$$\arg\min_{\boldsymbol{\Delta\sigma}} J(\boldsymbol{\Delta\sigma}) = \| \mathbf{H}\boldsymbol{\Delta\sigma} - \boldsymbol{\Delta\varepsilon} \|_{\mathbf{2}}^{\mathbf{2}} + \mathbf{G}_{\alpha}(\boldsymbol{\sigma}) \, . \quad (1)$$

Here, $\mathbf{H} \in \mathbb{R}^{m \times n}$ denotes the ray-path matrix, which discretizes the imaging domain into n pixels and encodes the accumulated path lengths contributing to each time-of-flight (ToF) values. The vector $\boldsymbol{\Delta\sigma} \in \mathbb{R}^n$ stores the difference between the conjectured ($\tilde{\boldsymbol{\sigma}}$) and solution ($\boldsymbol{\sigma}$) slowness (inverse of SoS) for each pixel or voxel. The m reliable ToF measurements are stored in $\boldsymbol{\Delta\varepsilon} \in \mathbb{R}^m$. The term $G_\alpha(\boldsymbol{\sigma})$ represents the regularization functional weighted by a scalar parameter α.

For a function $f(r) \in \mathbb{R}^n$, the Laplacian operator is the divergence of the gradient ($\nabla^2 f(r) = \nabla \cdot \nabla f(r)$). In order to introduce anisotropy, the following modified second-order spatial derivative operator is proposed:

$$\Phi(f(r)) = \nabla \cdot \mathbf{A} \nabla \mathbf{f}(\mathbf{r}) \, , \quad (2)$$

where $\mathbf{A} \in \mathbb{R}^{n \times n}$ is a diagonal matrix of directional regularization weights. The diagonal entries of $\mathbf{A}$, $\kappa_{f_i} \in \mathbb{R}^+ \cup \{0\}$, control the degree of smoothing in each spatial direction. For simplicity, it is assumed that these weights depend solely on the direction, not on spatial position.

In two dimensions, using standard finite-difference approximations, the discrete anisotropic operator $\mathbf{L}^{\mathbf{aniso}} \in \mathbb{R}^{n \times n}$ is defined as

$$\mathbf{L}^{\mathbf{aniso}}_{\mathbf{i,j}} = \begin{cases} -2(\kappa_x + \kappa_y) \, , & \text{if } j = \{i\} \\ \kappa_x \, , & \text{if } j = \{i-1, i+1\} \\ \kappa_y \, , & \text{if } j = \{i-n_x, i+n_x\} \\ 0 \, , & \text{otherwise .} \end{cases} , \quad (3)$$

where $n = n_x n_y$ is the total number of pixels, and n_x and n_y are the number of pixels along the x and y directions, respectively.

With prior knowledge of the solution, denoted as $\boldsymbol{\sigma}_{\text{prior}}$, the regularization term in Equation (1) becomes

$$G_\alpha(\boldsymbol{\sigma}) = \alpha \| \mathbf{L}^{\mathbf{aniso}} (\boldsymbol{\sigma} - \boldsymbol{\sigma}_{\mathbf{prior}}) \|_{\mathbf{2}}^{\mathbf{2}} \, . \quad (4)$$

When prior information indicates that SoS variations are directionally dependent —either globally or in a piecewise manner— the regularization weights can be adjusted accordingly. Increasing the regularization in a particular direction (e.g., x) tend to prevent solutions with large second derivatives yielding smoother transitions along that direction. Conversely, reducing the penalty allows solutions with greater second derivative and sharper variations in that direction. This mechanism helps guide the solution away from non-physical local minima and toward more plausible reconstructions.

To reduce the number of tunable parameters and maintain consistent regularization balance across directions, the constraint $\kappa_x + \kappa_y = 1$ may be imposed. Under this constraint, one can define $\kappa \equiv \kappa_y$, so that $\kappa_x = 1 - \kappa$. This formulation allows intuitive control over the anisotropy of the regularization by varying a single parameter κ. Table 1 summarizes the qualitative effects of varying κ relative to the isotropic case ($\kappa = 0.5$).

Table 1. Qualitative interpretation of the impact of anisotropic regularization compared to the isotropic case ($\kappa = 0.5$).

	Solution ∇_f		Smoothness	
κ	y	x	y	x
< 0.5	Larger	Smaller	Lower	Higher
> 0.5	Smaller	Larger	Higher	Lower

3. Materials and Methods

To evaluate the proposed anisotropic regularization technique and cardiac imaging with a single linear large transducer with sparse elements, a numerical simulation was performed using the k-Wave toolbox for MATLAB [7]. The simulation domain was defined as a 150×150 mm^2 area, discretized into a 660×660 pixels grid. To cover the entire cardiac region, a linear transducer array was modeled with a total length of 120 mm, consisting of 128 punctual elements spaced with a pitch of 0.9091 mm. Given the domain size and the need to avoid phase-wrapping while maintaining adequate spatial resolution, a central frequency of 1 MHz was selected for a 3-cycle Gaussian-modulated pulse. The temporal resolution was set to $\Delta t = 1.4384 \times 10^{-4}$ s.

The numerical phantom, shown in Figure 1, represents a simplified axial cross-section of the human thorax, closed on the heart region. It features anatomical components such as the left and right ventricles filled with blood (1580 m/s), myocardium (1560 m/s), lungs (1480 m/s), and connective tissue as the background (1520 m/s). Bone structures were not included in this preliminary study.

To enable TDE, scatterers were emulated by intro-

ducing small density variations over 10 % of the pixels randomly selected, following a normal distribution with mean $\mu_{density} = 1000\ kg/m^3$ and standard deviation $\sigma_{density} = 5\ kg/m^3$. Acoustic attenuation was neglected for this preliminary evaluation.

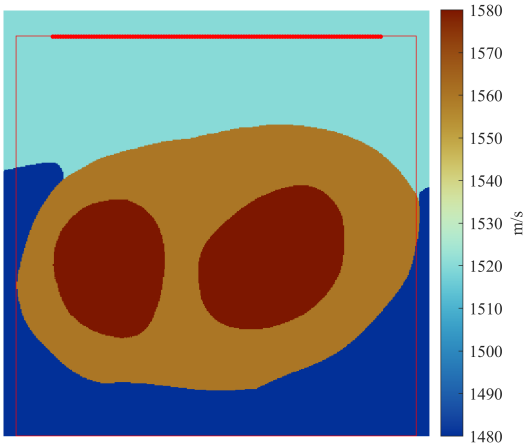

Figure 1. Cardiac simplified SoS numerical phantom.

The ROI for reconstruction, as indicated in Figure 1, is a square zone directly in front of the transducer array. The transducer elements, shown as small circles, appear as a thick line at the top of the ROI due to pixel size and element count.

The forward model, used to solve the inverse problem, assumed a homogeneous SoS and employed a straight-ray approximation to estimate the wavefront travel paths. The reconstruction algorithm was implemented in MATLAB using a stacked Conjugate Gradient for Least Squares (CGLS) method [8,9], iterated for 600 steps to ensure convergence.

The system matrix $\mathbf{H}$ was constructed by computing the intersections between straight-ray paths and the discretized grid, assigning the corresponding segment lengths to the appropriate matrix entries. Reconstructions were performed assuming a homogeneous prior slowness $\tilde{\sigma} = 1/1530\ s/m$, similar to the human body soft tissue average value admitted by commercial equipment manufacturers.

The SoS images were reconstructed on a coarser 65×65 grid. All simulation and reconstruction parameters were empirically tuned. The regularization weight was fixed at $\alpha = 0.20$ for all reconstructions. To limit the receiving aperture's directivity, an f-number of 0.75 was applied [10]. Additionally, a normalized cross-correlation threshold of 0.75 was used to assess the reliability of time-delay estimation (TDE) signals based on waveform similarity. The range of SoS values in the reconstructed images was defined by the minimum and maximum within each result. To study the influence of the anisotropic regularization parameter κ, values ranging from 0.00 to 1.00 in increments of 0.05 were tested. The reconstruction quality was quantitatively assessed using the root mean squared error (RMSE) metric.

4. Results and Discussion

Reconstructions of the numerical phantom using various values of the anisotropic coefficient κ, ranging from 0.10 to 0.80 in 0.10 increments, are shown in Figure 2. Each reconstructed image displays the corresponding κ value in the top-left corner. Quantitative RMSE results for all κ values are presented in Figure 3, including values for each anatomical structure as well as the overall reconstruction (denoted as total).

The lowest RMSE values were observed for κ values between 0.35 and 0.45, depending on the structure evaluated. Across all structures, reconstructions using anisotropic regularization outperformed the isotropic case ($\kappa = 0.5$).

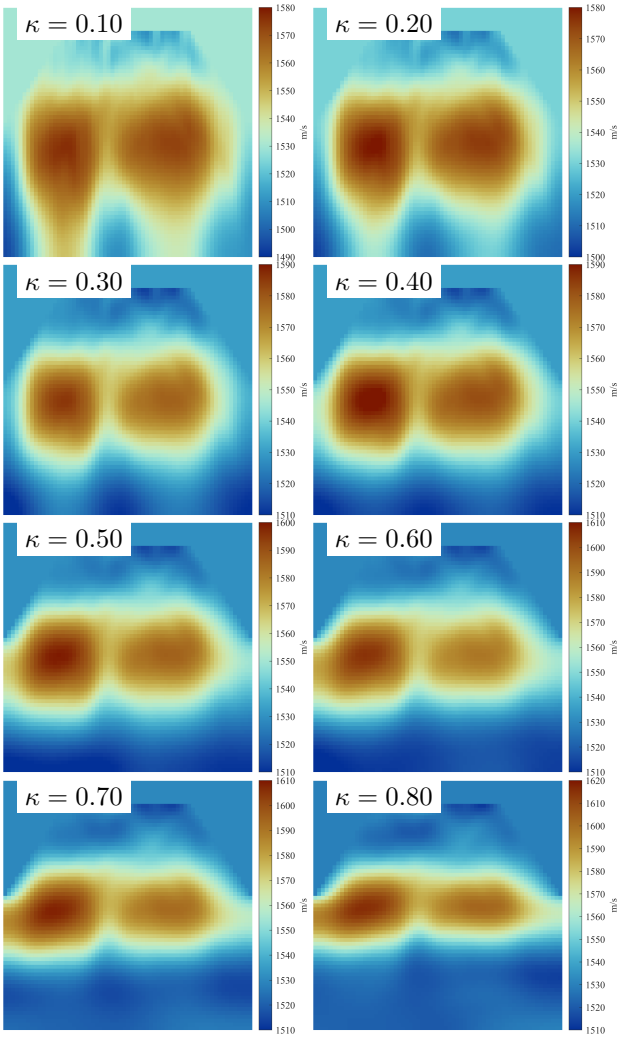

Figure 2. Speed-of-sound (SoS) reconstructions for some of the anisotropic coefficient values.

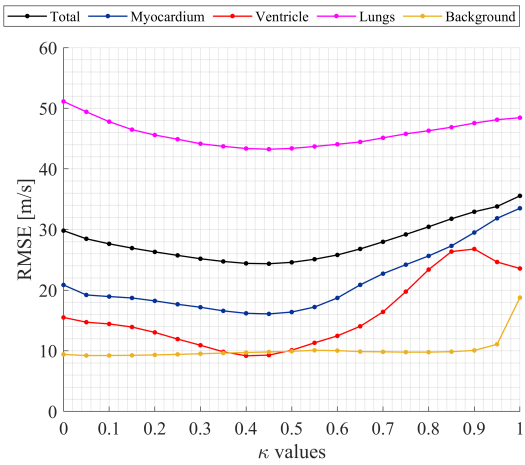

Figure 3. Root mean square error (RMSE) (m/s) by structure for all anisotropic coefficient values.

The myocardium and ventricular regions exhibited the best reconstruction quality when $\kappa = 0.45$. For $\kappa \geq 0.45$, the myocardium and ventricles (fully blood filled) regions experienced a noticeable degradation in accuracy, as reflected by a steep increase in RMSE. This behavior can be attributed to the anisotropic smoothing effect: as κ increases, regularization favors smoothing along the horizontal (y) direction.

While reconstructions obtained with $\kappa = 0.40$ and $\kappa = 0.50$ may appear visually similar, closer inspection reveals that smaller anisotropic values, within the range $0.35 \leq \kappa \leq 0.45$, better preserve the cross-sectional geometry of the heart. This observation is supported by the lowest RMSE values for both the myocardium and lungs occurring at $\kappa = 0.45$. For the ventricular regions, the lowest RMSE was achieved with $\kappa = 0.40$. This result aligns with expectations, as the ventricles are structurally similar and require reconstructions with reduced smoothing and higher gradients in the horizontal (y) direction to accurately delineate their boundaries.

5. Conclusion

This study proposed a Tikhonov regularization method with an anisotropic second-derivative operator to improve cardiac quantitative ultrasound imaging using a single large transducer. Results show that directionally dependent regularization enhances reconstruction both quantitatively and qualitatively, especially when incorporating expected axis-specific SoS contrast. These findings indicate the feasibility of quantitative cardiac SoS imaging with a single large-aperture transducer. Future work will validate the method experimentally, assess the realism of the simulations, and compare it with state-of-the-art approaches.

Acknowledgments

Roberto C. Ceccato acknowledges the financial support from the São Paulo Founding Agency FAPESP (Grant No. 2021/13997-0 and Grant No. 2023/15074-1). The Scientific colour map used in this study was developed by Crameri et al. [11].

References

[1] Ali R, Mitcham TM, Singh M, Doyley MM, Bouchard RR, Dahl JJ, Duric N. Sound speed estimation for distributed aberration correction in laterally varying media. IEEE Transactions on Computational Imaging 2023;9:367–382. ISSN 23339403.

[2] Jaëger M, Robinson E, Akarçay HG, Frenz M. Full correction for spatially distributed speed-of-sound in echo ultrasound based on measuring aberration delays via transmit beam steering. Physics in Medicine and Biology 6 2015; 60:4497–4515. ISSN 13616560.

[3] Sanabria SJ, Ozkan E, Rominger M, Goksel O. Spatial domain reconstruction for imaging speed-of-sound with pulse-echo ultrasound: Simulation and in vivo study. Physics in Medicine and Biology 10 2018;63. ISSN 13616560.

[4] Stähli P, Kuriakose M, Frenz M, Jaëger M. Improved forward model for quantitative pulse-echo speed-of-sound imaging. Ultrasonics 12 2020;108. ISSN 0041624X.

[5] Rau R, Schweizer D, Vishnevskiy V, Goksel O. Speed-of-sound imaging using diverging waves. International Journal of Computer Assisted Radiology and Surgery 7 2021; 16:1201–1211. ISSN 18616429.

[6] Sanabria SJ, Brevett T, Dahl J. Anisotropic regularization of ultrasound pulse-echo tomography for reconstruction of speed-of-sound and tissue heterogeneity through abdominal layers. In 2020 IEEE International Ultrasonics Symposium (IUS). IEEE. ISBN 978-1-7281-5448-0, 9 2020; 1–4.

[7] Treeby BE, Cox BT. k-wave: Matlab toolbox for the simulation and reconstruction of photoacoustic wave fields. Journal of Biomedical Optics 2010;15:021314. ISSN 10833668.

[8] Nocedal J, Wright SJ. Numerical Optimization. 2 edition. Springer New York, 12 2006. ISBN 978-0-387-30303-1.

[9] Aster RC, Borchers B, Thurber CH. Parameter Estimation and Inverse Problems. 3 edition. Elsevier, 2019. ISBN 978-0-12-804651-7.

[10] Perrot V, Polichetti M, Varray F, Garcia D. So you think you can DAS? a viewpoint on delay-and-sum beamforming. Ultrasonics 3 2021;111. ISSN 0041624X.

[11] Crameri F, Shephard GE, Heron PJ. The misuse of colour in science communication. Nature Communications 12 2020; 11. ISSN 20411723.

Address for correspondence:

Roberto C. Ceccato
Av. Prof. Luciano Gualberto, 158, 05508-010, São Paulo, Brazil
roberto.ceccato@usp.br